

Article

Autogenous Healing of Cracked Mortar Using Modified Steady-State Migration Test against Chloride Penetration

Fahad ul Rehman Abro ¹, Abdul Salam Buller ², Tariq Ali ³, Zain Ul-Abdin ^{4,5,*}, Zaheer Ahmed ⁶, Noor Ahmed Memon ⁷ and Ali Raza Lashari ¹

¹ Civil Engineering Department, Mehran University of Engineering and Technology, Jamshoro 76090, Pakistan; fahad.abro@gmail.com (F.u.R.A.); ali_raza1571@yahoo.com (A.R.L.)

² Civil Engineering Department, Larkana Campus, Quaid-e-Awam University of Engineering, Science and Technology, Larkana 77150, Pakistan; buller.salam@quest.edu.pk

³ Civil Engineering Department, The Islamia University of Bahawalpur, Bahawalpur 63100, Pakistan; tariqdehraj@gmail.com

⁴ Department of Civil Engineering, Ghent University, 609052 Ghent, Belgium

⁵ Tractebel (Engie), 1000 Brussels, Belgium

⁶ Civil Engineering Department, College of Engineering and Technology, University of Sargodha, Sargodha 40100, Pakistan; zaheer.ahmed@uos.edu.pk

⁷ Civil Engineering Department, Quaid-e-Awam University of Engineering, Science and Technology, Nawabshah 67450, Pakistan; nahmedmemon@gmail.com

* Correspondence: engineerzain14@gmail.com



Citation: Abro, F.u.R.; Buller, A.S.; Ali, T.; Ul-Abdin, Z.; Ahmed, Z.; Memon, N.A.; Lashari, A.R. Autogenous Healing of Cracked Mortar Using Modified Steady-State Migration Test against Chloride Penetration. *Sustainability* **2021**, *13*, 9519. <https://doi.org/10.3390/su13179519>

Academic Editors: Malindu Sandanayake, Zora Vrcelj and Rui Micaelo

Received: 16 June 2021

Accepted: 19 August 2021

Published: 24 August 2021

Publisher's Note: MDPI stays neutral with regard to jurisdictional claims in published maps and institutional affiliations.



Copyright: © 2021 by the authors. Licensee MDPI, Basel, Switzerland. This article is an open access article distributed under the terms and conditions of the Creative Commons Attribution (CC BY) license (<https://creativecommons.org/licenses/by/4.0/>).

Abstract: Concrete is a popular building material all over the world, but because of different physio-chemical processes, it is susceptible to crack development. One of the primary deterioration processes of reinforced concrete buildings is corrosion of steel bars within the concrete through these cracks. In this regard, a self-healing technique for crack repair would be the best solution to reduce the penetration of chloride ions inside concrete mass. In this study, a rapid chloride migration (RCM) test was conducted to determine the self-healing capacity of cracked mortar. With the help of the RCM test, the steady-state migration coefficient of cracked and uncracked specimens incorporating expansive and crystalline admixtures was calculated. Based on the rate of change of the chloride ion concentrations in the steady-state condition, the migration coefficient was calculated. Furthermore, bulk electrical conductivity tests were also conducted before and after the migration test to understand the self-healing behavior. It was evident from the test results that the self-healing of cracks was helpful to reduce the penetration of chloride ions and that it enhanced the ability of cracked mortar to restrict the chloride ingress. Using this test method, the self-healing capacity of the new self-healing technologies can be evaluated. The RCM test can be an acceptable technique to assess the self-healing ability of cement-based materials in a very short period, and the self-healing capacity can be characterized in terms of the decrease of chloride migration coefficients.

Keywords: chloride; crack; electrical conductivity; self-healing; steady-state migration

1. Introduction

Concrete is a global material used for construction projects because it is a relatively cheap material, and it is easy to use in construction. Concrete, as a matter of fact, is vulnerable to cracking, and these cracks generally develop in most concrete members considering the service life of the concrete. Therefore, these cracks can provide a quick way for chloride ions and carbonation to penetrate through the structure, which can lead to reinforcement corrosion causing failure of the structure [1]. Thus, to increase the service life of concrete, it is essential that these cracks may be repaired as quickly as possible to prevent harmful agents [2]. These cracks tend to spread, and new cracks frequently appear even after repair, resulting in a cycle of the ongoing degradation of concrete structure durability and a reduction in service life [3]. For the maintenance of these cracks, billions of dollars

are spent throughout the world. However, there are very few options available for making concrete constructions more resilient and sustainable [4].

To address this issue, researchers are looking for a solution based on the self-healing technique. The self-healing of cracks can increase the service life of the concrete by restricting the penetration of harmful agents through the cracks without involving any manual repairs [5]. Concrete itself can heal the cracks naturally up to a certain degree. When moisture is supplied to a cracked surface, it gets healed by the hydration of the unhydrated particles of the cement, thus forming calcium carbonate (CaCO_3). This process, however, will only heal the limited crack widths [4]. Recently, many research investigations have been undertaken over the last two decades to better understand various elements of intrinsic self-healing (SH) in concrete [6–15]. Moreover, some autonomous healing technologies utilizing super-absorbent polymers, encapsulated polymers, minerals, or bacteria are being studied [16–20].

Inorganic materials are very helpful to improve the self-healing capacity of cement-based materials with the help of rehydration of cement particles during the hydration process and the production of calcium carbonate because of the carbonation reaction of Ca^+ [1]. Sisomphon et al. [21] found that the cracks can also be healed by using the calcium sulfoaluminate (CSA) and crystalline admixtures which ettringite within the crack matrix.

Super absorbent polymers (SAPs) in a dry state can absorb water a thousand times greater than its dry weight. Upon concrete cracking when water enters the crack, these SAPs absorb the water and block the crack. SAPs are also known as internal curing agents, which means they are helpful for the hydration of unhydrated cement particles in the cement matrix. This hydration can also improve the performance of self-healing of the cracks [22–24]. Furthermore, the bacteria-based self-healing process works on the principle that the bacteria available in the concrete behaves as a catalyst and generates a precursor compound that can be used to make an appropriate filler material. The newly created compounds, such as calcium carbonate-based mineral precipitates, should then operate as a bio-cement, successfully sealing newly developed cracks [25].

By using the self-healing technique, the durability of the concrete structures can be improved. In this regard, the service life of the structures can be improved further, thereby saving the repair costs and time. In the preliminary phase of the self-healing concrete technology, limited research is available, and no standard method is available for the evaluation of the self-healing capacity of the different cement-based materials. To adopt self-healing in the practical field, the self-healing capacities of various technologies must be evaluated with the standard technique. Specifically, the micro-cracks (0–500 μm) have a direct impact on durability performance as compared to mechanical performance, so it is critical to assess the recovery of durability performance by self-healing. However, there has been little research on the durability of self-healing concrete. Commonly, durability is connected to indirect indications such as water absorption or permeability. An interlaboratory testing effort was recently used to assess pre-standard testing techniques for water permeability and absorption [26]. Water permeability or absorption testing techniques, on the other hand, have little effectiveness in determining direct resistance to chloride penetration. Very few articles are available in the literature to deal with the real durability in terms of chloride ingress and among those, a few on real reinforcement corrosion [2,27–29].

Peng et al. [28] numerically studied the effect of transverse crack self-healing on the corrosion rate of steel bars in concrete. For this purpose, they developed a deformed mesh model and also explored the dynamics of transverse cracking. They concluded that crack self-healing decreases the rate of chloride-ion diffusion into concrete as well as the rate of corrosion and surface potential of steel bars. Furthermore, Maes et al. [29] used polyurethane capsules to determine the autonomous self-healing capacity against the chloride penetration of cracked mortar using NT build 443 test methods [30]. When compared to uncracked mortar, the chloride diffusion coefficients in the zone immediately around the crack rose considerably. Improved resistance to chloride penetration was noticed for autonomous crack healing. Furthermore, an improvement of 100% was noticed in the

service life of cracked structures. For 200 μm , an improvement of 44 years was calculated based on the diffusion coefficient. However, this phenomenon was purely dependent on the healing mechanism they used; if the mechanism works perfectly, the cracks get sealed completely and a predicted service life can be achieved. Similarly, Azarsa et al. [31] used rapid chloride permeability, surface/bulk electrical resistivity, and water permeability tests to analyze the effect of crystalline admixtures on the concrete strength, durability performance, and self-healing effect. Results indicated that by adding the crystalline admixtures, the water permeability coefficient was reduced by three times, and the self-healing ratio was increased at a higher rate. Surface and bulk resistivity did not show any improvement when the crystalline admixtures were added. Moreover, Darquennes' [32] study suggested that early-age autogenous healing minimizes chloride penetration and enhances durability performance, especially in the case of blast furnace slag-containing specimens. Furthermore, it was concluded that the electrical migration test is a suitable method to observe the process of self-healing. However, it took two weeks to determine the diffusion coefficient of the healed specimens, which is a quite long time to determine the self-healing capacity of cracked specimens because the cracked specimens are always in contact with water (NaCl solution) and the chance of self-healing during the test is high. Sahmaran [33], then, used the test technique defined by ASTM C1202 [34] to study resistance to chloride penetration in specimens with crack widths ranging from 50 to 140 μm , and they evaluated the self-healing capacity after a healing age of 60 days. This method is used to evaluate chloride permeability in terms of charge passing through the pores of the specimens. In this method, an applied potential of 60 V is applied for 6 h, and the charge passed in terms of a coulomb is measured. This method is very short but cannot be used directly to determine chloride ion penetration because the charge passed through the concrete carries all ions including chloride ions. Since the electrical conductivity is dependent on the types and ion concentrations, this method is not reliable to calculate the self-healing capacity concerning chloride ion penetration. In this regard, Abro et al. [35] proposed a modified steady-state migration test method to determine the diffusion coefficient in a very short time (36 h) and used it to evaluate the self-healing capacity of crystalline and expansive materials. They modified the test method of ASTM C1202. An applied potential of 36 V was applied instead of 60 V in ASTM C1202, and the test duration was increased to 36 h to achieve the steady-state condition. The migration diffusion coefficient was calculated when the rate of drop of chloride ions was in a steady-state condition. Since 36 h is still a long period, it is encouraged to further reduce the test time.

This study aimed to propose a more appropriate method to evaluate the self-healing capacity of cracked concrete for the resistance to chloride penetration. For this purpose, the electrically-driven rapid migration test was employed to determine the diffusion coefficient of cracked mortars in a relatively short time. Besides, the bulk electrical conductivity of the specimens was measured before and after the migration test at every healing age. Furthermore, based on the calculated diffusion coefficient, a method to calculate the equivalent crack width after healing was proposed to analyze the recovery of chloride penetration in terms of crack width closure.

2. Experimental Program

2.1. Test Outline

Assessment of different degrees of self-healing of damaged sample were carried out by adding various types of admixtures with different percentages. There are two major parameters of this study: one is the crack size, ranging from 0 to 0.4, and the second is the dosage level of admixtures used. The steady-state migration test has been performed on the uncracked and cracked samples before and after healing (of 28, 56, and 120 days). The electrical conductivity of all the specimens was measured immediately before and after migration at all the healing ages.

2.2. Materials and Mix Proportions

Table 1 shows the mix proportions of various materials used in this study to produce mortar samples. Type I ordinary Portland cement and self-healing admixture with different proportions was used. Expansive agent Calcium Sulfoaluminate (CSA) was used as a self-healing material to heal the cracks, and a crystalline admixture of Na_2CO_3 was combined to accelerate the healing process. These materials were added with 2:1 ratio (CSA: Na_2CO_3) in the shape of granulated capsules having a size range of 0.6–1.2 mm. Three different percentages of 4%, 6%, and 8% by weight of sand were replaced. The details of mix proportions are tabulated in Table 1. 2.68 g/cm³ is the density of sand used for mixing. Table 1 depicts the values of slump flow and compressive strength at the end of 28-day curing.

Table 1. Details of the mix proportions and mortar properties.

Binder	Mixture Proportions (by Mass)					28-Day Compressive Strength (MPa)	Slump Flow (mm)
	Water	Cement	SH Materials % (2:1) CSA Na_2CO_3		Sand		
OPC	0.4	1	-		2	0.3	165
SH4	0.4	1	0.04		1.96	0.5	160
SH6	0.4	1	0.06		1.94	0.5	155
SH8	0.4	1	0.08		1.92	0.5	135

2.3. Specimen Preparations

After 24 h of mixing, all samples (Cylindrical Ø 100 mm \times 200 mm) were taken off from the molds. All specimens were then cut (central part) into pieces with a size of 50 mm at the end of the 28-day curing at a fixed temperature of 20 ± 2 °C in a water bath. Figure 1 depicts the complete procedure of specimen preparation. The specimens were split using a Brazilian splitting test as shown in Figure 1a. The specimen was kept in a specimen holder having rubber plates on top and bottom and was placed in the cracking jig under the unidirectional compression. After the specimens were split into two semicircles, the tapes of a specific thickness were put on the ends of the specimen to achieve the required thickness, as shown in Figure 1b. Finally, the two parts of the specimen were tied together by a steel band, as shown in Figure 1c [36].

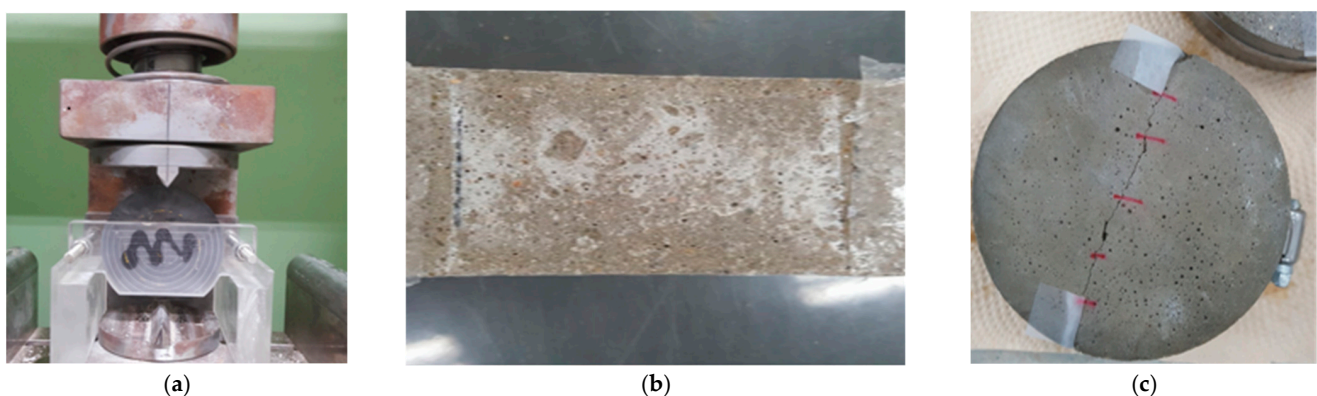


Figure 1. Preparation of cracked specimens; (a) splitting; (b) adhering silicon tapes; (c) reassembling.

Using an optical microscope, each cracked specimen was then checked for crack width determination; three points were located at each specimen on the top and bottom. Average values of the three points for each specimen were then considered as the final crack width of the specimen. The achieved and targeted crack widths of all specimens are given in Table 2. From Table 2, it is worth noting that the difference in targeted crack width and achieved crack width is less than 10%.

Table 2. Details of targeted and achieved crack widths.

Binder	Target Crack Width (μm)	Achieved Crack Width (μm)	Difference (%)
OPC	200	193	−3.5
	300	284	−5.3
	400	393	−1.8
SH4	200	188	−6.0
	300	273	−9.0
	400	378	−5.5
SH6	200	196	−2.0
	300	296	−1.3
	400	364	−9.0
SH8	200	201	0.5
	300	293	−2.3
	400	400	0.0

Self-healing capacity was evaluated initially before testing, then each specimen was kept in water bath at temperature of 20 ± 2 °C in order to trigger the self-healing mechanism until the other phase of testing started. The damaged specimen, having different mixture proportions, were placed for curing separately in order to prevent ion exchange among the specimen during testing. The cracked specimens were tested before self-healing, and then, to allow the self-healing process to continue, they were immersed in the water bath at a temperature of 20 ± 2 °C until the next test. The specimens with each mixture proportion were cured separately of the specimens with the other mixture proportions to prevent ion exchange between them.

2.4. Steady-State Chloride Migration Test

There are two methods that can determine the diffusion coefficient of the concrete using the electrical migration test. The first method calculates the migration coefficient under the non-steady-state condition NT build 492 [37], and the other calculates it under the steady-state condition which is NT build 355 [38]. In NT build 355, the electrically-driven migration test lasts for 1–2 weeks and the steady-state migration coefficient is calculated by using the Nernst–Planck equation. The rate of change of chloride ion concentration within a NaOH solution inside a cell is measured, and the migration coefficient is calculated when the ions reach the steady-state condition. However, the non-steady-state migration coefficient is measured by cutting the specimen into two semi-circles, and AgNO_3 is sprayed on the two halves. The change of color denotes the depth of chloride penetration [38] and the non-steady-state migration coefficient is calculated by using the equation proposed by Tang and Nilson [39], since it is quite difficult due to the rate of chloride transport through a fracture being too quick to assess the depth of chloride penetration in the crack. Hence, some researchers have employed the NT build 355 and ASTM C1202 test setups to evaluate the steady-state migration coefficient [32,35,40,41].

The Nernst–Planck equation defines the chloride flux in the diffusion cell as follows:

$$J_c = \frac{zF}{RT} Dc \frac{\partial U}{\partial x} \quad (1)$$

where J_c is the chloride flux, z is the ionic valence, F is the Faraday constant ($=96,485$ °C per equivalent), R is the gas constant ($=8.3145$ J/mol·K), T is the absolute temperature (K), D is the diffusion coefficient, c is the chloride concentration, U is the electrical potential applied (V), and x is the distance. If the applied potential is kept constant, then the diffusion coefficient in the steady-state condition can be determined by the following equation [39]:

$$D_{ssm} = \frac{RTL J_c}{zFU c_1} \quad (2)$$

where L is the specimen thickness (m), and c_1 is the chloride concentration in the upstream cell (catholyte). The following equation is used to determine the chloride flux under the steady state during the test:

$$J_c = \frac{V}{A} \left| \frac{\Delta c_1}{\Delta t} \right| = \frac{V}{A} \left| \frac{\Delta c_2}{\Delta t} \right| \quad (3)$$

where A is the cross-sectional area (m^2) through which ions pass, V is the volume of the upstream or downstream cell (m^3), and c_2 is the chloride concentration in the downstream cell (anolyte). Since under the steady-state condition, the rate of chloride drop is almost the same in the upstream cell as in the downstream cell, the diffusion coefficient can be calculated by the following equation:

$$D_{ssm} = \frac{RTL}{zFU} \frac{V}{A} \frac{1}{c_1} \left| \frac{\Delta c_1}{\Delta t} \right| = \frac{RTL}{zFU} \frac{V}{A} \left| \frac{\Delta \ln(c_1)}{\Delta t} \right| \quad (4)$$

The self-healing capacities of cracked specimens incorporating admixtures were evaluated. The test setup proposed by Abro et al. [35] was used. The upstream cell was filled with 0.5 M NaCl solution and the downstream cell with 0.3 M NaOH solution. Under the potential difference of 36 V, the chloride ion concentration in the upstream cell was measured for 24 h with an ion-selective electrode at an interval of 60 min for an initial 6 h and 120 min for the remaining 18 h. Each specimen was kept between two cells with a rubber seal to make sure that there was no leakage. Figure 2 depicts the schematic diagram and photography of the test setup.



Figure 2. Test setup for chloride migration test; (a) schematic diagram [36]; (b) pictorial view of the test setup.

Prior to testing, vacuumed air was removed from the pores of each damaged specimen in a desiccator for 12 h so that every specimen would be fully saturated with water. A room with a fixed humidity of $60 \pm 5\%$ and temperature of $20 \pm 2^\circ\text{C}$ was selected for testing.

An ion-selective electrode technique, Thermo Scientific ISE, produced by Orien [42], was used to quantify the chloride ion concentration in the upstream cell periodically, depending on the correlation between the potential achieved by ISE and the given chloride concentration for the initial six hours at an interval of 1 h. This is because change in the rate of change of the chloride concentration interval for reading was adjusted, and at every measurement, a small amount of liquid of chloride from upstream was taken off with a pipet.

2.5. Electrical Conductivity

Non-destructive electrical conductivity measurement was performed on $\Phi 100 \times 50$ mm disk specimens before and after the electrical migration test at every healing age.

The test was repeated three times on the specimen and the average was considered. Because of the polarization effect of the electrodes, measuring resistance with a DC signal is not suggested [43]. The current was applied through the specimen using an alternating current (AC) at a fixed frequency of 1 kHz. Previous research has shown that when the frequency is at least 1 kHz, the polarization effects in the material may be ignored [44,45]. The electrodes are circular stainless-steel plates with a contact sponge soaked in a weak soap solution placed between two electrodes to guarantee that the entire surface is in electrolytic contact with the electrode. Figure 3 illustrates a schematic diagram and test setup of the underlying physics involved in BR measurement.

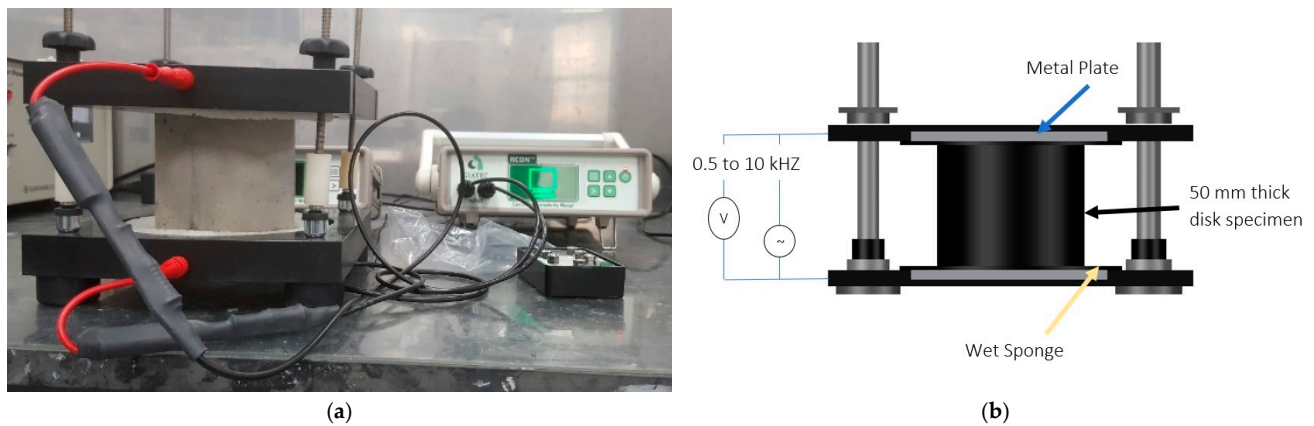


Figure 3. The test setup of electrical conductivity; (a) test setup; (b) schematic diagram.

3. Results and Discussion

3.1. Effect of Self-Healing Materials on the Crack Healing

In the beginning, as depicted in Figure 4, the migration test was repeated before healing on the same specimen in different cycles to check the repeatability. In first cycle, all the specimens were uncracked; in 2nd cycle, the first specimen was uncracked and all three were 0.2 mm cracked; in 3rd cycle, the last two specimens were 0.3 mm cracked while the first two were uncracked and 0.2 mm cracked; and in last cycle, uncracked, 0.2 mm, 0.3 mm, and 0.4 mm cracked specimens were used for the migration test, and the same were tested at 28-, 56-, and 120-day healing. The calculated coefficients of variation (COVs) in the migration coefficient of uncracked specimen are 11.43%, 6.66%, 9.78%, and 11.07% for OPC, SH4, SH6, and SH8 mixes, respectively, while the same for the 0.2 mm cracked specimens are 9.10%, 2.26%, 5.23%, and 5.85% for OPC, SH4, SH6, and SH8 mixes, respectively.

The chloride concentration in the upstream cell for the cracked and uncracked specimens of different mixes was measured with the help of an ion-selective electrode which is depicted in Figure 5. It is evident in Figure 5 that rate of drop in chloride concentration is larger for cracked specimens than for uncracked specimens. However, after a healing period of 28 days and 56 days, the drop in chloride concentration is reduced for all the specimens. This improvement is small in the uncracked specimen as compared to cracked specimens because after healing, the cracked specimens are healed, and the amount of resistance to chloride penetration is larger than the uncracked specimens, especially those mixes containing self-healing materials.

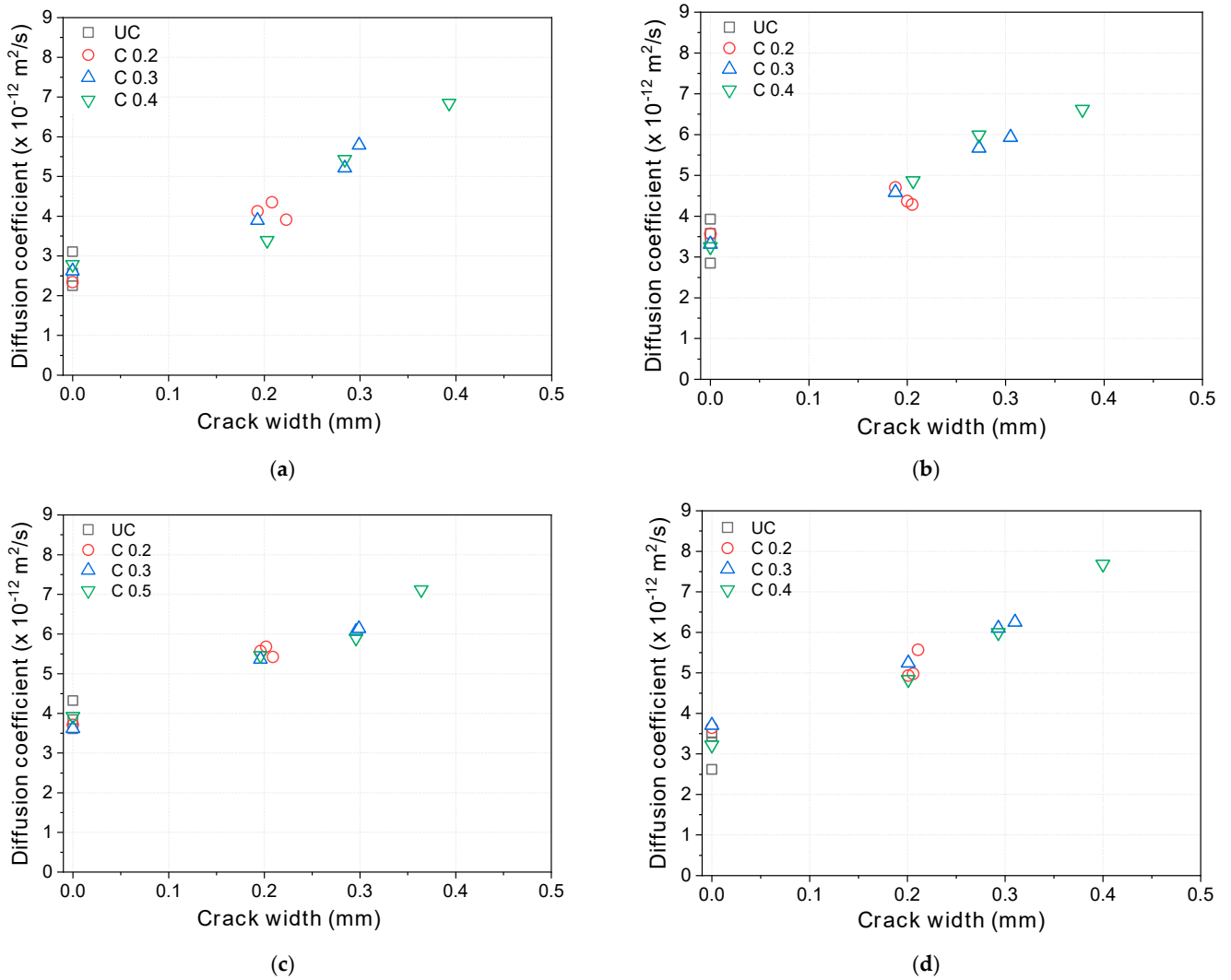


Figure 4. Relationship of crack width and migration coefficients before healing; (a) OPC; (b) SH4; (c) SH6; (d) SH8.

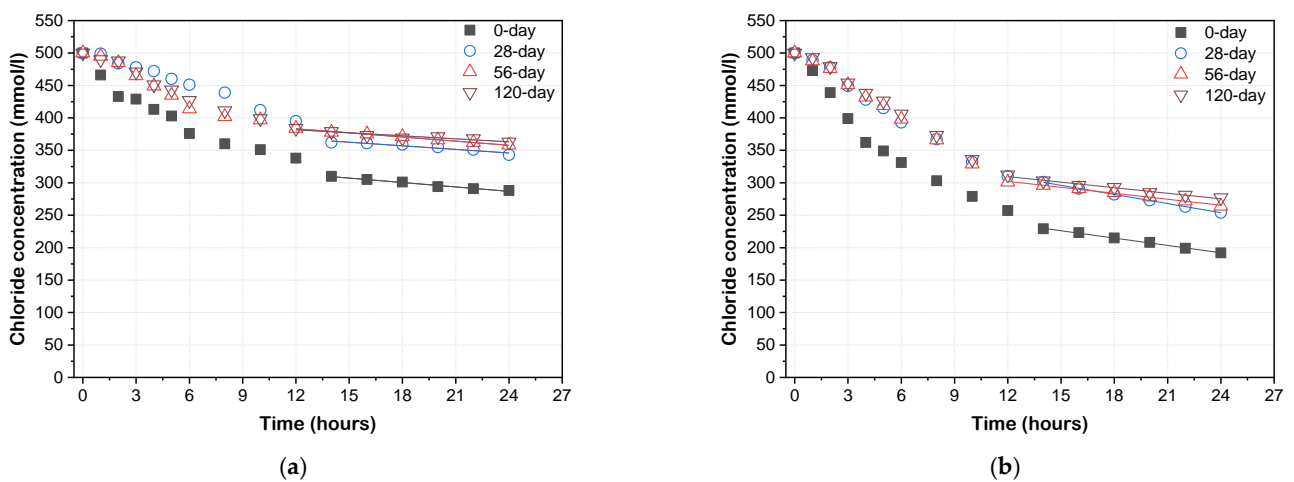


Figure 5. Cont.

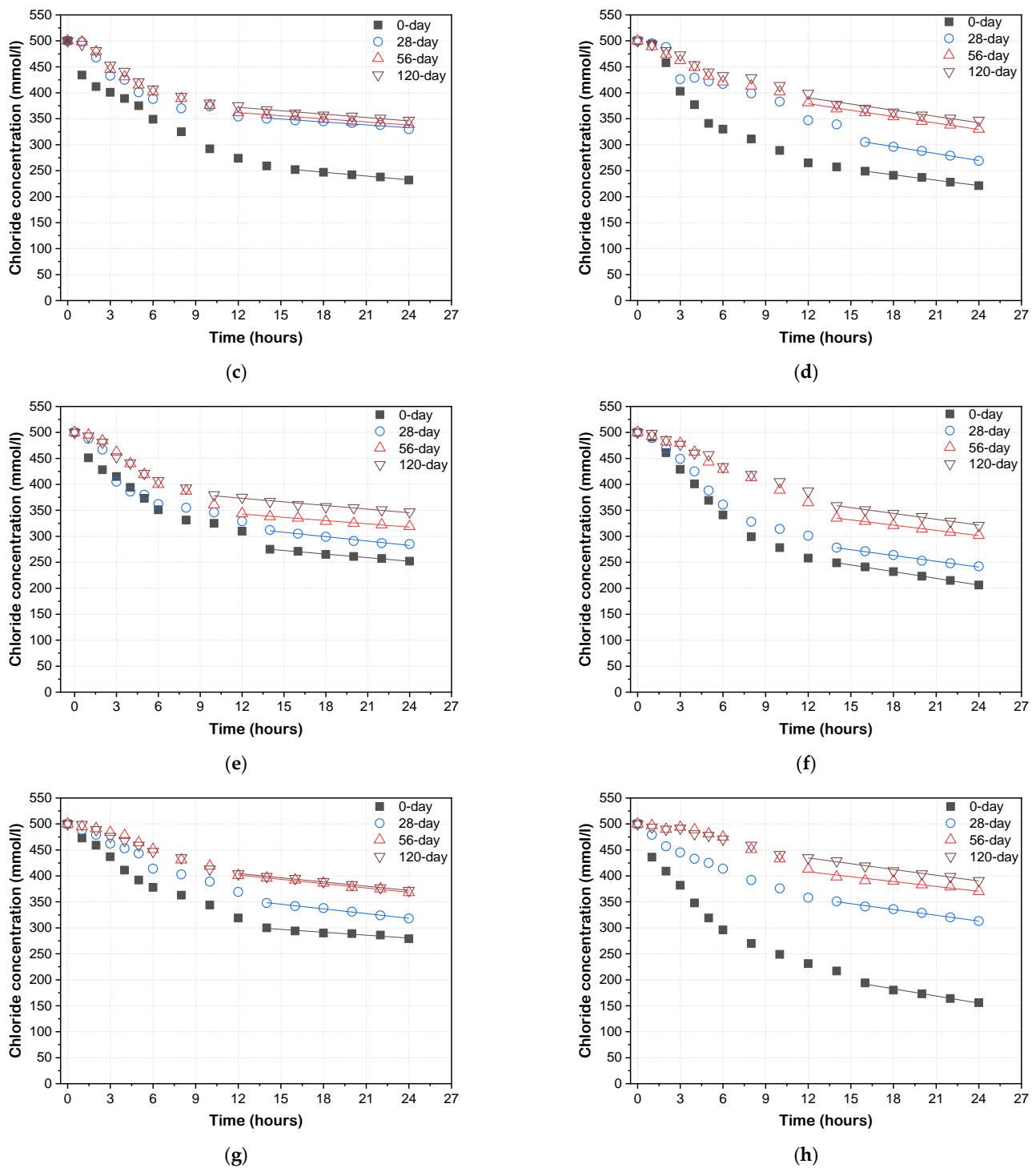


Figure 5. Rate of drop in chloride concentration; (a) OPC uncracked; (b) OPC 0.4 mm cracked; (c) SH4 uncracked; (d) SH4 0.4 mm cracked; (e) SH6 uncracked; (f) SH6 0.4 mm cracked; (g) SH8 uncracked; (h) SH8 0.4 mm cracked.

This phenomenon can be understood with the help of calculated migration coefficients. The steady-state migration coefficients were calculated before and after healing by using Equation (4). Figure 6 represents the calculated migration coefficients concerning healing ages for different cracked specimens. Figure 6 illustrates that the higher the crack width, the higher the migration coefficients are, because the crack provides a passage for chloride ions to penetrate easily. As the healing period progresses, the migration coefficient decreases. In the case of low cracked specimens (near 0.2 mm cracked) after the 120-day healing period,

the migration coefficient decreases in such a way that it is almost equivalent to an uncracked specimen without considering the mixture. The larger crack widths (0.3 and 0.4 mm) are completely dependent on the type of mixture. It could be seen for SH8 mix that after 120-day healing, the reduction % for all specimens as compared to 56-day healing is better, especially for the 0.3 mm cracked specimen. In the case of OPC specimen, the reduction percentages for the migration coefficient after 120-day healing are 21.4%, 26.1%, 24.9%, and 19% for un-cracked (UC), 0.2 mm, 0.3 mm, and 0.4 mm cracked specimens, respectively. The same for the SH4 mix are 26.8%, 35.3%, 34.7.3%, and 25.8% for UC, 0.2 mm, 0.3 mm, and 0.4 mm cracked specimens, respectively. Those for the SH6 mix are 26.3%, 43.7%, 40.7%, and 32.8% for UC, 0.2 mm, 0.3 mm, and 0.4 mm cracked specimens, respectively.

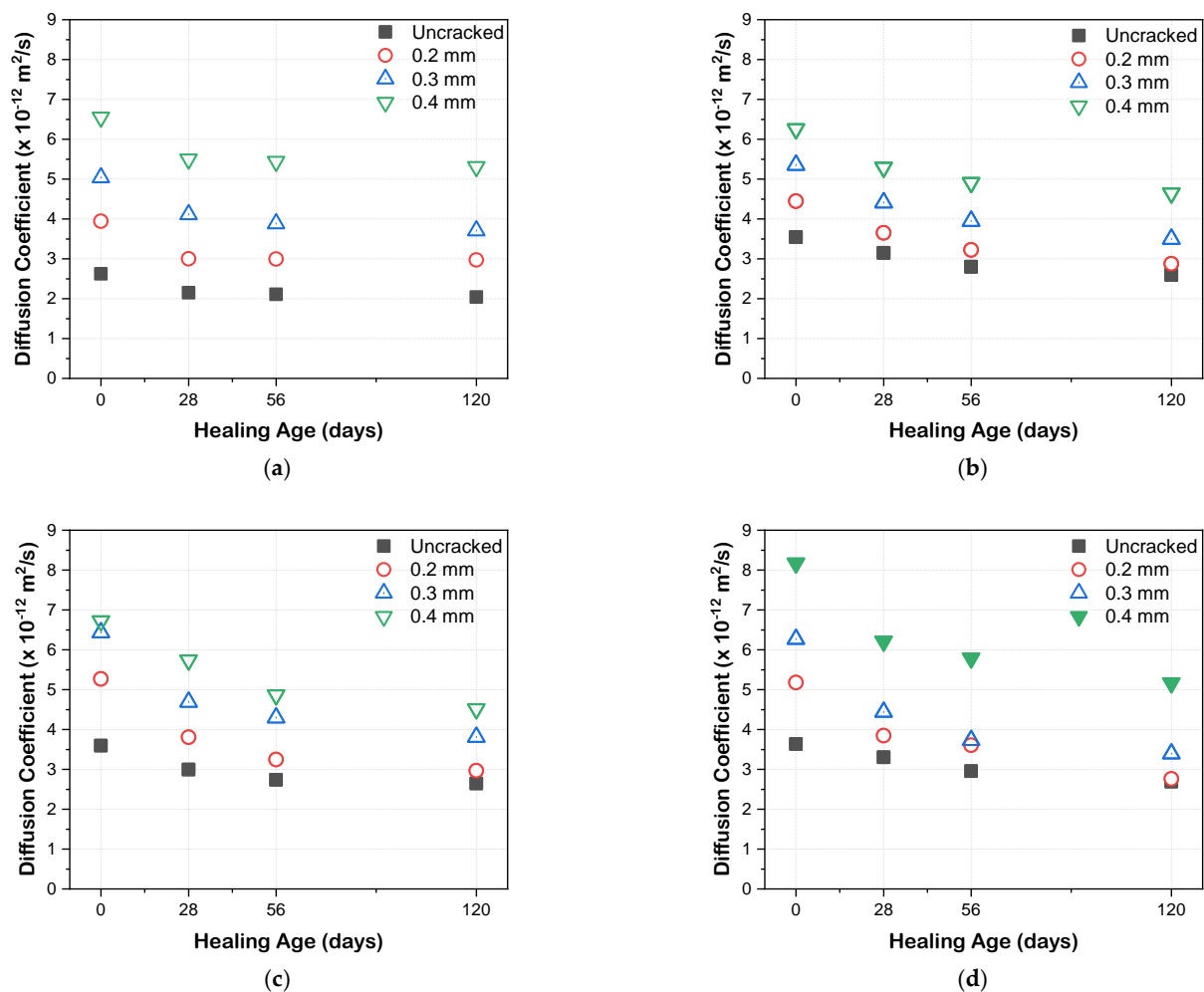


Figure 6. Calculated migration coefficients for different mixes; (a) OPC; (b) SH4; (c) SH6; (d) SH8.

The same for the SH8 mix are 26.0%, 37.8%, 45.9%, and 36.8% for UC, 0.2 mm, 0.3 mm, and 0.4 mm cracked specimens, respectively. The numbers show that as the percentage of healing material is increased, the amount of reduction rate increases. The expansive agent (CSA) along with crystal admixtures present in the special mix is supposed to create ettringite by the hydration process. As the percentage of healing material is increased, it is expected that the amount of ettringite produced by the hydration process would be increased. This increased amount helps to heal the cracks, block the harmful agents, and increases the durability of concrete.

3.2. Index of Self-Healing Capacity and Equivalent Crack Width

Furthermore, the self-healing capacity was also calculated using the index proposed by Abro et al. [35]. They proposed an index to quantitatively calculate the self-healing capacity

for the different self-healing materials based on the steady-state migration coefficient calculated by the steady-state migration test. The migration coefficient of the cracked specimen generally decreases with age. This phenomenon assumes that self-healing material is generated on the cracked surface, and the crack width is reduced.

It is understood that in the steady-state condition, a damaged sample can be the cracked specimen and can be signified into parts—i.e., the uncracked part and the cracked part. In this condition, the total ionic flow can be written as:

$$Q_{tot} = Q_{ucr} + Q_{cr} \quad (5)$$

where Q_{ucr} is the ionic flow through mortar (kg/s) and Q_{cr} is the ionic flow through the crack (kg/s). The quantity of ionic material that crosses through a certain area per unit of time, Equation (5), can be rewritten as:

$$J_{tot} A_{tot} = J_{ucr} A_{ucr} + J_{cr} A_{cr} \quad (6)$$

Then, since $J = D \partial c / \partial x$:

$$D_{eq} \frac{\partial c}{\partial x} A_{tot} = D_{ucr} \frac{\partial c}{\partial x} A_{ucr} + D_{cr} \frac{\partial c}{\partial x} A_{cr} \quad (7)$$

where D_{eq} is the equivalent migration coefficient of chloride in the cracked mortar (m^2/s), A_{tot} is the total surface area including crack, perpendicular to the direction of flow (m^2), D_{ucr} and D_{cr} are the migration coefficient of chloride in the uncracked zone and the crack (m^2/s), respectively, and A_{ucr} and A_{cr} are the surface area of the uncracked zone and the crack perpendicular to the direction of flow [m^2], correspondingly. Because the cracked area is too small, it can be assumed that $A_{tot} \approx A_{ucr}$, and Equation (7) becomes:

$$D_{cr} A_{cr} = (D_{eq} - D_{ucr}) A_{tot} \quad (8)$$

Based on resistance to chloride penetration, the self-healing index can be given as under:

$$SH_c(t) = 1 - \frac{Q_{cr}(t)}{Q_{cr,i}} = 1 - \frac{D_{cr}(t) A_{cr}(t)}{D_{cr,i} A_{cr,i}} = 1 - \frac{[D_{eq}(t) - D_{ucr}(t)] A_{tot}}{[D_{eq,i} - D_{ucr,i}] A_{tot}} \quad (9)$$

$$\therefore SH_c(t) = 1 - \frac{D_{eq}(t) - D_{ucr}(t)}{D_{eq,i} - D_{ucr,i}}$$

where $Q_{cr}(t)$ and $Q_{cr,i}$ are the ionic flow at healing age t and initial stage, respectively (kg/s). $D_{eq}(t)$, $D_{cr}(t)$, and $D_{ucr}(t)$ are the equivalent migration coefficient of cracked mortar, the migration coefficient through the crack, and the migration coefficient of uncracked mortar at healing age t (m^2/s), respectively. $D_{eq,i}$, $D_{ucr,i}$, and $D_{ucr,i}$ are the migration coefficients at the initial stage (m^2/s). The total area A_{tot} is constant. $A_{cr}(t)$ and $A_{cr,i}$ are the area of crack perpendicular to the exposure surface at healing age t and initial stage, respectively.

At age t , if the difference in migration coefficient between cracked and uncracked specimens is the same as the initial one, the self-healing capacity will be 0%, and if the migration coefficients of cracked and uncracked specimens are same at age t , then SH_c will be 100%, which means that the crack face is completely healed.

Figure 7 illustrates the calculated self-healing capacities for different mixes based on the calculated migration coefficients. From the figure, it can be noticed that the amount of healing is larger in low-cracked (0.2 mm) specimens. Healing of 91.5% in the case of the SH8 mix for 0.2 mm cracked can be seen, which suggests that the crack is almost filled, whereas for 0.4 mm cracked specimens, the healing amount is below 50% in all cases. This suggests that the healing materials are capable of healing the cracks of limited widths as in the case of 0.3 mm, a suitable recovery of 73.4% has been achieved in case SH8.

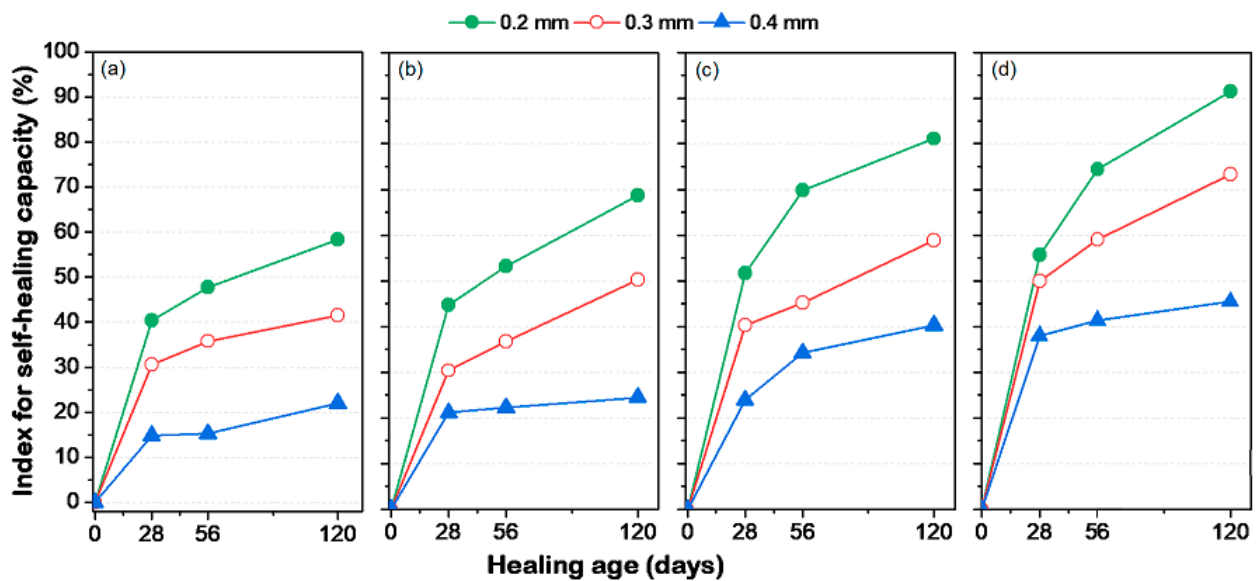


Figure 7. Calculated index for self-healing capacity for different mixes; (a) OPC; (b) SH4; (c) SH6; (d) SH8.

In 2011, Jang et al. [41] proved that the migration coefficient does not increase with an increase of crack width up to $80 \mu\text{m}$. A technique of equivalent crack width was proposed in the current study. From Figure 8, the procedure of determining the equivalent crack width is defined. According to the literature [32,41], the migration coefficient increases linearly as crack width is increased.

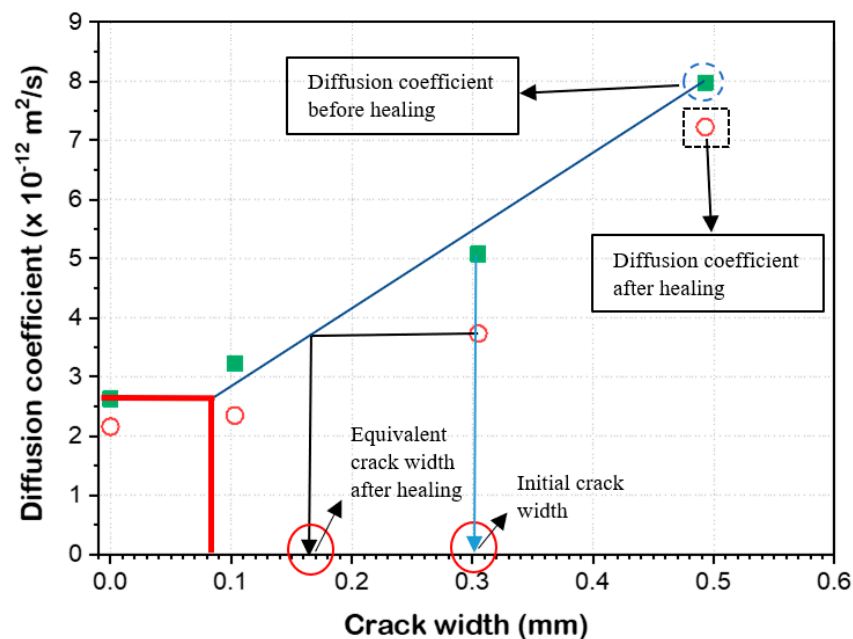


Figure 8. Procedure to determine the equivalent crack width.

After healing, the migration coefficient of the cracked specimens decreased, and those are equated with the migration coefficient at 0-day healing; the crack width of the healed specimen is also determined, as shown in Figure 8. The values of determined equivalent crack widths are presented in Table 3. $W_{cr,i}$ is the initial crack width of the specimen before healing, and $W_{cr(t)}$ is the equivalent crack width after the healing age of the specimen.

Table 3. Summary of the calculated crack widths at different healing ages.

Mix ID	$W_{cr,i}$ (μm)	$W_{cr,28-d}$ (μm)	$W_{cr,56-d}$ (μm)	$W_{cr,120-d}$ (μm)
OPC	193	121	107	95
	284	194	182	170
	393	251	261	230
SH4	188	121	107	95
	273	190	135	80
	378	269	239	210
SH6	196	108	≤ 80	≤ 80
	296	162	138	105
	364	248	172	158
SH8	201	130	≤ 80	≤ 80
	293	200	130	105
	400	290	260	240

3.3. Electrical Conductivity Test Results

Electrical conductivity of the uncracked and cracked specimens of all mixtures was conducted at the healing ages of 28, 56, and 120 days. The electrical conductivity (EC) was conducted before starting the migration test and immediately at the end of the migration test to understand the effect of healing during the migration tests. Usually, as the concrete got older, resistivity enhanced because of the continuous hydration of cement, also due to the setting of the cement. The reliance of the resistivity of cement on its microstructure properties, just as the conductivity of its pore arrangement, demonstrates an increment in resistivity after some time since cement's interconnected pore network diminishes and OH particles in the pore arrangement are burned through, attributing to a reduction in its conductivity. Initially, the preliminary test was conducted to understand the effect of height on the EC measurements. Tests were conducted on cylindrical specimens having a size of $\varnothing 100 \times 200$ mm. The test time was 1 min, the interval was set to 5 s, and the test was repeated three times on each specimen. After completing the test on $\varnothing 100 \times 200$ mm specimen, the same specimen was cut to 100 mm length, cutting a 50 mm part from both sides, and in the same way, resistivity of the specimen was measured three times. In the end, the same specimen was again cut to $\varnothing 100 \times 200$ mm, cutting 25 mm from both sides of the specimen, and the specimen was then tested for the resistivity tests. Figure 9 shows the schematic diagram and the complete process of cutting and testing the specimen.

Table 4 presents the results of the average electrical conductivity measurements for OPC specimens. From the results, it can be seen that the average results are almost near each other.

Table 4. Preliminary electrical conductivity results.

Specimen Length (mm)	Test No.	Electrical Conductivity (mS/s)	Mean	Standard Deviation	Coefficient of Variation (%)
200	1	24.50	24.32	0.17	0.70
	2	24.31			
	3	24.16			
100	1	26.08	25.98	0.086	0.33
	2	25.97			
	3	25.91			
50	1	24.97	25.13	0.152	0.60
	2	25.16			
	3	25.27			

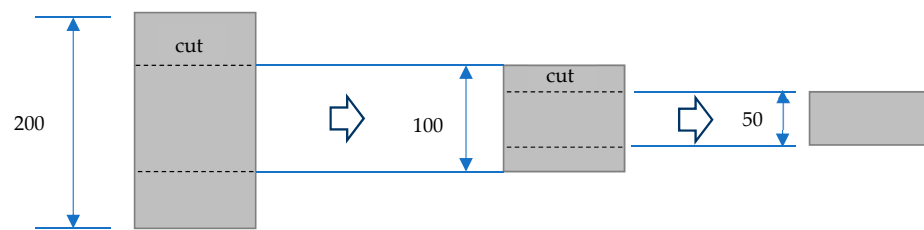


Figure 9. Schematic view of the preliminary cutting of specimen.

Figure 10 presents the calculated EC results. EC was measured before and after migration tests at every healing age to check if there was any self-healing during the migration tests. It was done mainly because during the migration tests the specimens were intact with water for 24 h. Overall, the margin of EC results before and after migration is very little except for two specimens, SH6—0.4 mm crack and SH4 uncracked, which is likely due to the manual error moistness of sponge of the conductivity meter. Furthermore, it can be noticed that in comparison with the migration test, EC results shows a reduction up to 56 days of healing. After 56-day healing, when it comes to 120-day healing, the amount of healing in terms of EC is very marginal except those for SH8 mixes. This probably is due to the larger percentage of healing materials used which continues the hydration process for a very long time and reduces the pores available in the microstructure of specimens. The available pores are the main pathway for the chloride ions to penetrate through the concrete. By and large, cements containing translucent admixtures did not show any significant differences in improving electrical conductivity when contrasted with control combinations. It ought to be noticed that estimating concrete electrical conductivity is a roundabout testing procedure to obtain data about its penetrability which probably will not be a fitting method to comprehend the mending conduct of broad and glasslike materials under penetration or diffusion. Accordingly, this examination likewise explored other toughness assessment strategies to make some far-reaching determinations about the parts of utilizing CA and costly specialists, or to figure out which procedure can really address the ability of the mending materials utilized in the current investigation.

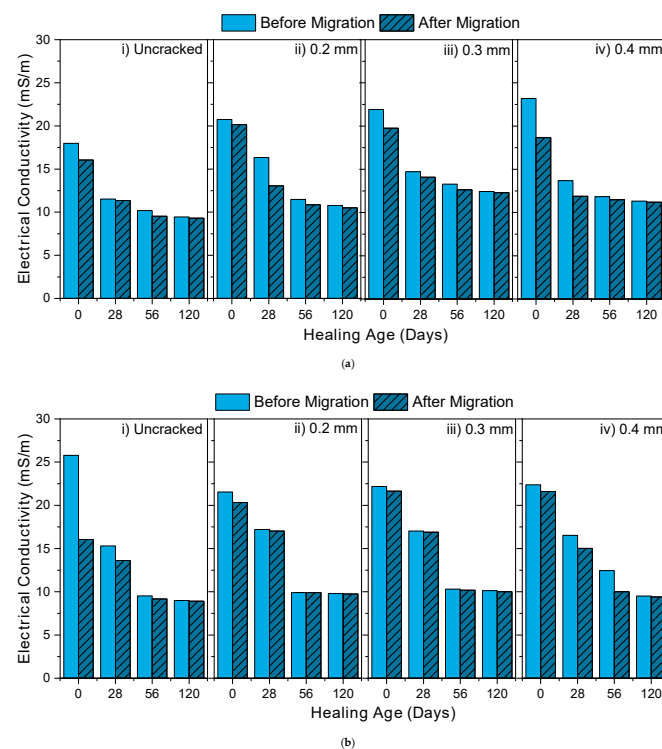


Figure 10. Cont.

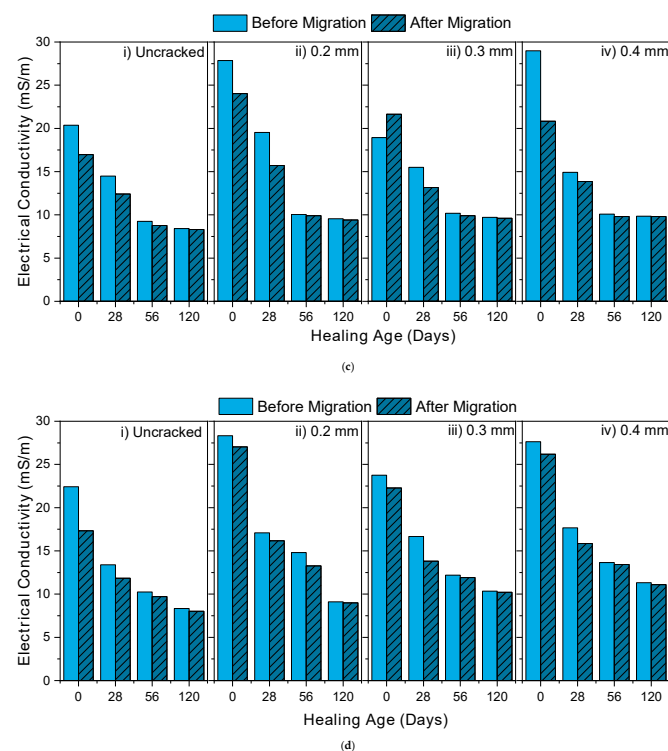


Figure 10. Representation of electrical conductivity with respect to healing age; (a) OPC; (b) SH4; (c) SH6; (d) SH8.

4. Conclusions

In the current study, the self-healing capacity of cracked mortar containing crystalline admixtures (CA) and expansive agents was investigated against the penetration of chloride ions with the help of a modified steady-state migration test. For that reason, chloride diffusivity and electrical conductivity were investigated. Based on the results obtained in this study, the following conclusions can be drawn:

1. The proposed modified migration test method is a suitable method that can be used to examine the degree of self-healing of the cracked mortars in a very short time. The degree of self-healing of the crack is strongly associated to the crack width, the type of mortar, and the healing age.
2. For the cracked specimens with 0 day(s) of healing, the transport properties are highly modified for all the specimens irrespective of their materials. It will not be wrong to say that the main parameter which influences the chloride penetration at an early age is the crack width, regardless of material.
3. There is a strong linear relationship between crack width and chloride migration coefficients. The total chloride diffusion has multiplied when the specimen has large crack width because the chloride diffusion in crack is much faster than in mortar.
4. The equivalent crack width is effective to evaluate the suitability of self-healing technology, whether the crack width after self-healing is smaller than the target crack width of the structure, such as allowable crack width by design code. It is possible to compare the self-healing performance with the degree of self-healing quantitatively.
5. The electrical conductivity of concrete is an indirect test method for determining its permeability, which does not give accurate information about the healing process of the different cement-based materials. It also depends upon the moisture available in the pores of specimens, which is quite critical.

Author Contributions: Conceptualization, F.u.R.A. and A.S.B.; methodology, F.u.R.A. and Z.U.-A.; software Z.A.; validation, F.u.R.A. and A.S.B.; formal analysis, T.A.; investigation, A.S.B.; resources, A.S.B.; data curation, A.S.B.; writing—original draft preparation, F.u.R.A.; writing—review and editing, A.S.B. and Z.U.-A.; visualization, A.R.L.; supervision, F.u.R.A.; project administration, N.A.M. All authors have read and agreed to the published version of the manuscript.

Funding: All authors certify that they have no affiliations with or involvement in any organization or entity with any financial interest or non-financial interest in the subject matter or materials discussed in this manuscript.

Institutional Review Board Statement: Not applicable.

Informed Consent Statement: Not applicable.

Data Availability Statement: The data presented in this study are available on request from the corresponding author.

Conflicts of Interest: The authors declare no conflict of interest.

References

1. Yoo, K.; Jang, S.; Lee, K.-M. Recovery of Chloride Penetration Resistance of Cement-Based Composites Due to Self-Healing of Cracks. *Materials* **2021**, *14*, 2501. [[CrossRef](#)]
2. Van Belleghem, B.; Kessler, S.; van den Heede, P.; van Tittelboom, K.; de Belie, N. Chloride induced reinforcement corrosion behavior in self-healing concrete with encapsulated polyurethane. *Cem. Concr. Res.* **2018**, *113*, 130–139. [[CrossRef](#)]
3. Van Tittelboom, K.; De Belie, N. Self-healing in cementitious materials—A review. *Materials* **2013**, *6*, 2182–2217. [[CrossRef](#)]
4. Azarsa, P.; Gupta, R.; Biparva, A. Assessment of self-healing and durability parameters of concretes incorporating crystalline admixtures and Portland Limestone Cement. *Cem. Concr. Compos.* **2019**, *99*, 17–31. [[CrossRef](#)]
5. Roig-Flores, M.; Pirritano, F.; Serna, P.; Ferrara, L. Effect of crystalline admixtures on the self-healing capability of early-age concrete studied by means of permeability and crack closing tests. *Constr. Build. Mater.* **2016**, *114*, 447–457. [[CrossRef](#)]
6. Li, M.; Li, V.C. Cracking and Healing of Engineered Cementitious Composites under Chloride Environment. *ACI Mater. J.* **2011**, *108*, 333–340. [[CrossRef](#)]
7. Şahmaran, M.; Keskin, S.B.; Ozerkan, G.; Yaman, I.O. Self-healing of mechanically-loaded self consolidating concretes with high volumes of fly ash. *Cem. Concr. Compos.* **2008**, *30*, 872–879. [[CrossRef](#)]
8. Reinhardt, H.-W.; Jooss, M. Permeability and self-healing of cracked concrete as a function of temperature and crack width. *Cem. Concr. Res.* **2003**, *33*, 981–985. [[CrossRef](#)]
9. Granger, S.; Loukili, A.; Pijaudier-Cabot, G.; Chanvillard, G. Experimental characterization of the self-healing of cracks in an ultra high performance cementitious material: Mechanical tests and acoustic emission analysis. *Cem. Concr. Res.* **2007**, *37*, 519–527. [[CrossRef](#)]
10. Hearn, N. Self-sealing, autogenous healing and continued hydration: What is the difference? *Mater. Struct.* **1998**, *31*, 563–567. [[CrossRef](#)]
11. Jacobsen, S.; Sellevold, E.J. Self healing of high strength concrete after deterioration by freeze/thaw. *Cem. Concr. Res.* **1996**, *26*, 55–62. [[CrossRef](#)]
12. Aldea, C.-M.; Song, W.-J.; Popovics, J.S.; Shah, S.P. Extent of healing of cracked normal strength concrete. *J. Mater. Civ. Eng.* **2000**, *12*, 92–96. [[CrossRef](#)]
13. Sahmaran, M.; Li, M.; Li, V.C. Transport properties of engineered cementitious composites under chloride exposure. *ACI Mater. J.* **2007**, *104*, 604–611.
14. Jacobsen, S.; Marchand, J.; Boisvert, L. Effect of cracking and healing on chloride transport in OPC concrete. *Cem. Concr. Res.* **1996**, *26*, 869–881. [[CrossRef](#)]
15. Buller, A.S.; Abro, F.U.R.; Lee, K.-M.; Jang, S.Y. Mechanical recovery of cracked fiber-reinforced mortar incorporating crystalline admixture, expansive agent, and geopolymer. *Adv. Mater. Sci. Eng.* **2019**, *2019*, 3420349. [[CrossRef](#)]
16. Lee, H.; Wong, H.; Buenfeld, N. Self-sealing of cracks in concrete using superabsorbent polymers. *Cem. Concr. Res.* **2016**, *79*, 194–208. [[CrossRef](#)]
17. Ferrara, L.; Van Mullem, T.; Alonso, M.C.; Antonaci, P.; Borg, R.P.; Cuenca, E.; Jefferson, A.; Ng, P.; Peled, A.; Roig-Flores, M.; et al. Experimental characterization of the self-healing capacity of cement based materials and its effects on the material performance: A state of the art report by COST Action SARCOS WG2. *Constr. Build. Mater.* **2018**, *167*, 115–142. [[CrossRef](#)]
18. Souradeep, G.; Kua, H.W. Encapsulation technology and techniques in self-healing concrete. *J. Mater. Civ. Eng.* **2016**, *28*, 04016165. [[CrossRef](#)]
19. De Belie, N.; Gruyaert, E.; Al-Tabbaa, A.; Antonaci, P.; Baera, C.; Bajare, D.; Darquennes, A.; Davies, R.; Ferrara, L.; Jefferson, T.; et al. A review of self-healing concrete for damage management of structures. *Adv. Mater. Interfaces* **2018**, *5*, 1800074. [[CrossRef](#)]
20. Buller, A.S.; Abro, F.-R.; Ali, T.; Jakhrani, S.H.; Ul-Abdin, Z. Stimulated autogenous-healing capacity of fiber-reinforced mortar incorporating healing agents for recovery against fracture and mechanical properties. *Mater. Sci.* **2021**. [[CrossRef](#)]

21. Sisomphon, K.; Copuroglu, O.; Koenders, E. Effect of exposure conditions on self healing behavior of strain hardening cementitious composites incorporating various cementitious materials. *Constr. Build. Mater.* **2013**, *42*, 217–224. [[CrossRef](#)]
22. Kang, S.-H.; Hong, S.-G.; Moon, J. Absorption kinetics of superabsorbent polymers (SAP) in various cement-based solutions. *Cem. Concr. Res.* **2017**, *97*, 73–83. [[CrossRef](#)]
23. Mechtcherine, V.; Wyrzykowski, M.; Schröfl, C.; Snoeck, D.; Lura, P.; De Belie, N.; Mignon, A.; Van Vlierberghe, S.; Klemm, A.J.; Almeida, F.C.R.; et al. Application of super absorbent polymers (SAP) in concrete construction—Update of RILEM state-of-the-art report. *Mater. Struct.* **2021**, *54*. [[CrossRef](#)]
24. Tenório Filho, J.R.; Mannekens, E.; van Tittelboom, K.; van Vlierberghe, S.; de Belie, N.; Snoeck, D. Innovative SuperAbsorbent Polymers (iSAPs) to construct crack-free reinforced concrete walls: An in-field large-scale testing campaign. *J. Build. Eng.* **2021**, *43*, 102639. [[CrossRef](#)]
25. Mors, R.M.; Jonkers, H.M. Bacteria-based self-healing concrete—An introduction. In Proceedings of the V International PhD Student Workshop on Durability of Reinforced Concrete; From Composition to Service Life Design, Espoo, Finland, 9–10 February 2012; pp. 32–39.
26. Van Mullem, T.; Anglani, G.; Dudek, M.; Vanoutrive, H.; Bumanis, G.; Litina, C.; Kwiecień, A.; Al-Tabbaa, A.; Bajare, D.; Stryzewska, T.; et al. Addressing the need for standardization of test methods for self-healing concrete: An inter-laboratory study on concrete with macrocapsules. *Sci. Technol. Adv. Mater.* **2020**, *21*, 661–682. [[CrossRef](#)] [[PubMed](#)]
27. De Belie, N.; Van Belleghem, B.; Erşan, Y.Ç.; van Tittelboom, K. Durability of self-healing concrete. *MATEC Web Conf.* **2019**, *289*, 01003. [[CrossRef](#)]
28. Peng, C.; Wu, Q.; Shen, J.; Mo, R.; Xu, J. Numerical study on the effect of transverse crack self-healing on the corrosion rate of steel bar in concrete. *J. Build. Eng.* **2021**, *41*, 102767. [[CrossRef](#)]
29. Maes, M.; van Tittelboom, K.; de Belie, N. The efficiency of self-healing cementitious materials by means of encapsulated polyurethane in chloride containing environments. *Constr. Build. Mater.* **2014**, *71*, 528–537. [[CrossRef](#)]
30. Nordtest. *Concrete, Hardened: Accelerated Chloride Penetration (NT BUILD 443)*; Nordtest Method; Nordtest: Serravalle Scrivia, Italy, 1995.
31. Van den Heede, P.; van Belleghem, B.; Araújo, M.A.; Feiteira, J.; de Belie, N. Screening of different encapsulated polymer-based healing agents for chloride exposed self-healing concrete using chloride migration tests. *Key Eng. Mater.* **2018**, *761*, 152–158. [[CrossRef](#)]
32. Darquennes, A.; Olivier, K.; Benboudjema, F.; Gagné, R. Self-healing at early-age, a way to improve the chloride resistance of blast-furnace slag cementitious materials. *Constr. Build. Mater.* **2016**, *113*, 1017–1028. [[CrossRef](#)]
33. Şahmaran, M. Effect of flexure induced transverse crack and self-healing on chloride diffusivity of reinforced mortar. *J. Mater. Sci.* **2007**, *42*, 9131–9136. [[CrossRef](#)]
34. ASTM C1202. *Standard Test Method for Electrical Indication of Concrete 's Ability to Resist Chloride*; ASTM: West Conshohocken, PA, USA, 1981; pp. 1–6. [[CrossRef](#)]
35. Abro, F.R.; Buller, A.S.; Lee, K.-M.; Jang, S.Y. Using the steady-state chloride migration test to evaluate the self-healing capacity of cracked mortars containing crystalline, expansive, and swelling admixtures. *Materials* **2019**, *12*, 1865. [[CrossRef](#)] [[PubMed](#)]
36. Shin, K.J.; Bae, W.; Choi, S.-W.; Son, M.; Lee, K.M. Parameters influencing water permeability coefficient of cracked concrete specimens. *Constr. Build. Mater.* **2017**, *151*, 907–915. [[CrossRef](#)]
37. Nordtest. *Chloride Migration Coefficient from Non-Steady-State Migration Experiments (NT Build 492)*; Nordtest Method; Nordtest: Serravalle Scrivia, Italy, 1999.
38. Nordtest. *Concrete, Mortar and Cement-Based Repair Materials: Chloride Diffusion Coefficient from Migration Cell Experiments (NT Build 355)*; Nordtest Method; Nordtest: Espoo, Finland, 1997.
39. Tang, L.; Nilsson, L.-O. Rapid determination of the chloride diffusivity in concrete by applying an electrical field. *ACI Mater. J.* **1993**, *89*, 49–53.
40. Sahmaran, M.; Yildirim, G.; Erdem, T.K. Self-healing capability of cementitious composites incorporating different supplementary cementitious materials. *Cem. Concr. Compos.* **2013**, *35*, 89–101. [[CrossRef](#)]
41. Jang, S.Y.; Kim, B.S.; Oh, B.H. Effect of crack width on chloride diffusion coefficients of concrete by steady-state migration tests. *Cem. Concr. Res.* **2011**, *41*, 9–19. [[CrossRef](#)]
42. Thermo Fisher Scientific. *User Guide Chloride Ion Selective Electrode*; Thermo Fisher Scientific: Waltham, MA, USA, 2008.
43. AASHTO TP-95-11. *Standard Test Method for Surface Resistivity of Concrete's Ability to Resist Chloride Ion Penetration*; American Association of State Highway and Transportation Officials: Washington, DC, USA, 2011; Volume 4.
44. Yildirim, G.; Aras, G.H.; Banyhussan, Q.; Şahmaran, M.; Lachemi, M. Estimating the self-healing capability of cementitious composites through non-destructive electrical-based monitoring. *NDT E Int.* **2015**, *76*, 26–37. [[CrossRef](#)]
45. Al-Dahawi, A.; Sarwary, M.H.; Öztürk, O.; Yildirim, G.; Akin, A.; Şahmaran, M.; Lachemi, M. Electrical percolation threshold of cementitious composites possessing self-sensing functionality incorporating different carbon-based materials. *Smart Mater. Struct.* **2016**, *25*, 105005. [[CrossRef](#)]